Ab Initio Study of the HF($X^1\Sigma_g^+$)−H(^2S) van der Waals Complex

Vladimír Lukeš,*,† Imrich Vrábel,‡,§ Viliam Laurinc,† and Stanislav Biskupič§

Department of Chemical Physics, Slovak University of Technology, Radlinského 9, SK-81 237 Bratislava, Slovak Republic, Institute of Theoretical Chemistry and Molecular Biology, University of Vienna, Währingerstrasse 17, AT-1100 Vienna, Austria, and Department of Physical Chemistry, Slovak University of Technology, Radlinského 9, SK-81 237 Bratislava, Slovak Republic

Received: February 14, 2001; In Final Form: May 21, 2001

The adiabatic potential energy surface (PES) of the HF($X\ ^1\Sigma_g^+$)−H(^2S) van der Waals complex, described by Jacobi coordinates ($r = 0.918$ Å, R, Θ), was investigated using the supermolecular unrestricted fourth-order Møller−Plesset perturbation theory. Our calculations indicate two minima for the linear arrangements. The primary minimum was found for the H···HF geometry at $R = 3.13$ Å with a well depth of $D_e = 98.01$ cm^{-1} and the secondary one for the H···FH orientation at $R = 3.21$ Å with a well depth of $D_e = 31.36$ cm^{-1}. The presented PES reveals that these minima are separated by a barrier of 81.73 cm^{-1} (with respect to the primary minimum) at $R = 3.17$ Å and $\Theta = 99°$. The physical origin of the studied weak interaction was analyzed by the intermolecular perturbation theory on the basis of the single determinant UHF wave function. The separation of the interaction energy shows that the locations of the predicted stable structures are primarily determined by the anisotropy of the repulsive Heitler−London exchange−penetration and attractive dispersion + induction energy components. Dynamical calculations have also been performed to determine the bound states of the studied complex. They show that the ground state is 21.01 cm^{-1} below the dissociation to HF($X\ ^1\Sigma_g^+$) + H(^2S).

1. Introduction

A knowledge of the inter- and intramolecular potential energy surfaces (PES) is essential for the understanding of many physical, chemical, and biological processes as well as for intrinsic properties of molecules or their clusters. The main experimental sources of information on PES are the high-resolution spectroscopic studies[1−4] as well as scattering experiments.[5−9] In contrast to the weakly bonded neutral clusters containing the closed-shell molecules, such experimental data are less frequent for the neutral open-shell complexes.[10−19] However, the forces acting between a pair of open-shell and closed-shell atoms or molecules are interesting from the chemical point of view, as they exhibit high reactivity and appear as transient intermediates in the reactions.[20] Furthermore, as was shown by Heaven,[11] these complexes offer a unique opportunity to bridge the gap between a weak van der Waals (vdW) interaction and an incipient chemical bond. In addition, since the seminal work of Rebentrost and Lester,[21] the dynamics of reaction between open-shell atoms and hydrogen halide (HX) molecules has served as an important model problem for understanding the role of long-range forces in the scattering processes.

The reaction of fluorine atoms with hydrogen molecules is one of the most extensively studied elementary chemical reactions, mainly because of its importance in H_2/F_2 chemical laser.[22] High-resolution molecular beam experiments by Neumark et al.[23,24] yielded vibrationally state resolved differential cross sections for the F + H_2. These cornerstone experiments have been followed by others in which the ultimate rovibrational resolution of the products has been achieved. Among the most important works of recent years, we should also mention the molecular beam experiments[25−27] on the F + D_2 isotropic variant of the reaction, the photodetachment experiments on the FH_2^- ion,[28,29] and the studies on the F + H_2 reaction.[30−33]

On the theoretical side, the advent of high quality ab initio calculations by Truhlar and co-workers[34,35] and by Werner and co-workers[36,37] during the 1990s has allowed, for the first time, the reproduction of most of the experimental observables by exact quantum mechanical reactive scattering calculations. Stark and Werner[36] also gave a useful summary of the early theoretical works on the FH_2 system. It is evident from their brief survey that most theoretical studies of this chemical reaction have used interaction potentials designed to reproduce the transition state region, with relatively little attention being paid to the long-range behavior. Maierle et al.[38] and also Takayanagi and Kurosaki[39,40] showed that the attractive vdW well has an important effect on the reactive scattering, especially on the location of reactive scattering resonances. Recently, Dobbyn et al.[41] have extended these works with using the higher-level ab initio calculations.

It can be expected that the PES for the FH_2 reactive system contains a minimum at long range, which could support bound states. It should be possible to observe the spectra of the vdW complex and use them to learn about the long-range intermolecular forces. In fact, such spectra might provide a detailed probe of the entrance or exit valleys of the chemical reaction. However, the reliable experimental studies appear to be problematic. This is not fully unexpected, because the fluorine molecule as well as the hydrogen atom is troublesome to work with, because of its natural intrinsic corrosiveness and reactivity. Additionally, at present, there is no suitable evidence of the

* To whom correspondence should be addressed.
† Department of Chemical Physics, Slovak University of Technology.
‡ University of Vienna, Währingerstrasse.
§ Department of Physical Chemistry, Slovak University of Technology.

10.1021/jp010583e CCC: $20.00
Published on Web 07/19/2001

frequency ranges in which such spectra might be found or the pattern of energy levels that might be expected.

In this case, the determination of the ab initio PES accompanied by bound state calculations[42,43] can provide valuable assistance in the prediction of spectroscopic observations for this system. However, even with recent advances in ab initio techniques, the construction of reliable PES for such open-shell systems is rather difficult. The theoretical description of open-shell vdW complexes has been dominated by nonperturbative supermolecular methods, such as the coupled electron pair approximation or MR−CI, because they enable calculations of excited states of different symmetries and multiplicities. However, in multireference theoretical descriptions, it is not easy to ensure the unambiguous correction to the basis set superposition error (BSSE).[44−46] Fortunately, these difficulties can be bypassed by the supermolecular unrestricted Møller−Plesset perturbation theory (UMPPT) based on the single determinant reference. The efficiency of the UMPPT accompanied by the intermolecular perturbation theory (I−PT) has recently been established for several open-shell vdW systems, in particular He(^{1}S)−O_2 ($X^3\Sigma_g^-$),[47,48] Ar(^{1}S)−NH($X^3\Sigma_g^-$),[49] He(^{1}S)−CH($X\ ^2\Pi$),[50] He(^{1}S)−Cl(^{2}P),[51] He(^{1}S)−H(^{2}S),[48] Ne(^{1}S)−CN($X\ ^2\Sigma^+$),[52] and H(^{2}S)−F_2($X\ ^1\Sigma_g^+$).[53]

With respect to the previous theoretical studies, the main goal of this paper is to provide a detailed BSSE-free characterization of the PES of HF($X\ ^1\Sigma_g^+$)−H(^{2}S) complex using supermolecular UMP4 theory. In this context, the origin of the stability of the PES minima will be analyzed using the I−PT based on the single-determinant UHF reference wave function. Finally, the results of the bound-state calculations will be discussed.

2. Methodology and Definitions

To investigate the weak interaction within the radical vdW system, we will use the standard ab initio supermolecular approach. At a given level of theory, the interaction energy is calculated from the expression

$$\Delta E_{\mathrm{int}}^{(n)} = E_{\mathrm{AB}}^{(n)} - E_{\mathrm{A}}^{(n)} - E_{\mathrm{B}}^{(n)} \qquad n = \mathrm{UHF},\ 2,\ 3,\ 4,\ \ldots \tag{1}$$

where E_{AB} is the energy of the supersystem AB and E_{A} (E_{B}) tends for the energy of the noninteracting monomer A (B). The level of theory is indicated by the superscript index "*n*", e.g., $\Delta E_{\mathrm{int}}^{(2)}$ denotes the UMP2 interaction energy.

To analyze the supermolecular results, the interpretative tools based on the intermolecular perturbation theory (I−PT) are applied at the SCF as well as at the post-HF theoretical levels.[46,54−59]

The UHF−SCF interaction energy can be decomposed as follows:

$$\Delta E^{\mathrm{UHF}} = \Delta E^{\mathrm{HL}} + \Delta E_{\mathrm{def}}^{\mathrm{UHF}} \tag{2}$$

where ΔE^{HL} is the Heitler−London (HL) energy[60] and $\Delta E_{\mathrm{def}}^{\mathrm{UHF}}$ represents the UHF deformation contribution.[46] According to the I−PT defined in the orthogonalized basis sets,[57−59,61] ΔE^{HL} may be further divided into the first-order Hartree−Fock electrostatic $E_{\mathrm{els}}^{(100)}$ (for the notation of this and further perturbation terms see, e.g., ref 54) and HL exchange-penetration $\Delta E_{\mathrm{exch}}^{\mathrm{HL}}$ components

$$\Delta E^{\mathrm{HL}} = \Delta E_{\mathrm{exch}}^{\mathrm{HL}} + E_{\mathrm{els}}^{(100)} \tag{3}$$

It should be mentioned that the first-order exchange energy ($E_{\mathrm{exch}}^{(100)}$) may also be defined within the framework of the symmetry adapted perturbation theory (SAPT).[56] This term differs from the $\Delta E_{\mathrm{exch}}^{\mathrm{HL}}$ by a small SAPT zero-order exchange term, vanishing when the dimer-centered basis set (DCBS) is used in the calculations.[55]

The UHF deformation energy originates from the mutual electric polarization effects. This term might be approximated using the sum of the following two perturbation terms: $E_{\mathrm{ind}}^{(200)}$ and $E_{\mathrm{exch-ind}}^{(200)}$ (second-order UHF Coulombic and SAPT exchange induction energies).[59] However, the inclusion of the higher order perturbation contributions and the response or orbital-relaxation effects is necessary at shorter intermolecular distances.[62,63]

Similarly to the closed-shell cases, the second-order UMP2 correlation interaction energy can be partitioned as

$$\Delta E_{\mathrm{int}}^{(2)} = E_{\mathrm{els}}^{(12)} + E_{\mathrm{disp}}^{(200)} + E_{\mathrm{exch-disp}}^{(200)} + \Delta E_{\mathrm{other}}^{(2)} \tag{4}$$

where $E_{\mathrm{els}}^{(12)}$ denotes the second-order electrostatic correlation energy (containing $E_{\mathrm{els}}^{(102)}$ and $E_{\mathrm{els}}^{(120)}$ energies[64]). $E_{\mathrm{disp}}^{(200)}$ and $E_{\mathrm{exch-disp}}^{(200)}$ represent the second-order Hartree−Fock Coulombic[65] and SAPT exchange dispersion energies.[56] $\Delta E_{\mathrm{other}}^{(2)}$ encompasses the remaining exchange and deformation correlation corrections as well as the response effects.[54,62]

Using the diagrammatic techniques, it is easy to separate the third-order dispersion-correlation ($E_{\mathrm{disp}}^{(210)}$, $E_{\mathrm{disp}}^{(201)}$) energy and the Hartree−Fock third-order dispersion ($E_{\mathrm{disp}}^{(300)}$) energy.[54,48] However, the complete physical interpretation of the higher than second-order contributions of the interaction electron-correlation energies is not straightforward.

3. Calculation Details

All I−PT calculations were performed by our own program codes interfaced to the Gaussian 94 program package.[66] The supermolecular BSSE was determined via the counterpoise method of Boys and Bernardi.[45] The presented UHF interaction energy terms were calculated using dimer-centered basis sets of the constituent monomers.[46] The evaluation of the SAPT second-order exchange-induction and exchange-dispersion energies at the UHF level was realized in the framework of the single-exchange approximation (the quadratic and higher orders of the overlap integrals were neglected.).[56] The HL energy was obtained using the standard Gram−Schmidt orthogonalization procedure.

A system of Jacobi coordinates (r, R, Θ) was used in all our calculations. The coordinates r, R, and Θ represent in turn the intramolecular H−F distance, the distance from H to the center of mass of HF, and the Jacobi angle between R and the vector from the hydrogen to the fluorine atom. If this convention is used, $\theta = 0°$ denotes the linear orientation H···HF, whereas $\theta = 180°$ designates the opposite linear H···FH geometry. In this work, the r distance was kept at the value of 0.918 Å which represents the equilibrium bond distance of the HF molecule in its ground state.[67] It is a reasonable approximation, because, in the work of Stark and Werner,[36] it was shown that the equilibrium geometry of HF molecule is negligibly affected by the interacting H atom.

The augmented correlation consistent triple-ζ basis set (aug-cc-pVTZ) has been used throughout this study.[68,69] It has been extended with a set of midbond functions [3s3p2d] of Tao and Pan[70] (with the exponents *s*, *p*: 1.8, 0.6, 0.2; *d*: 1.2, 0.3). These bond functions were fixed at the center of the axis defined by the interacting hydrogen atom and the center of mass of the HF. The corresponding extended sets are hereafter denoted as

TABLE 1: UMP4/Aug-cc-pVTZ+bf PES of the HF($X^1\Sigma_g^+$)−H(^{2}S) Complex[a]

R (Å)	$\theta = 0°$	$\theta = 20°$	$\theta = 40°$	$\theta = 60°$	$\theta = 70°$	$\theta = 80°$	$\theta = 90°$	$\theta = 100°$	$\theta = 120°$	$\theta = 140°$	$\theta = 160°$	$\theta = 180°$
2.50	1246.0	1148.7	982.6	840.8	793.5	767.0	757.3	756.2	747.4	704.1	646.4	619.9
2.55	859.2	810.6	728.9	640.9	609.8	592.1	585.9	585.1	574.3	532.9	480.2	456.2
2.60	546.1	535.4	514.9	475.0	457.0	446.7	443.3	442.7	430.8	392.0	344.2	322.6
2.70	95.7	135.4	201.9	226.2	227.0	227.2	228.0	228.1	215.9	182.7	144.2	127.2
2.80	−181.1	−114.7	−0.6	61.5	73.9	80.6	84.1	84.6	73.5	46.1	15.9	2.7
2.90	−339.2	−261.4	−125.3	−43.4	−24.4	−14.0	−9.1	−8.1	−17.7	−39.6	−62.9	−73.0
3.00	−418.1	−338.1	−196.4	−106.6	−84.4	−72.2	−66.4	−65.2	−73.1	−90.4	−108.1	−115.6
3.10	−445.5	−368.8	−231.2	−140.9	−118.1	−105.3	−99.2	−97.8	−104.2	−117.5	−130.8	−136.2
3.20	−440.5	−370.2	−242.2	−156.2	−133.9	−121.3	−115.3	−113.9	−118.8	−129.0	−138.8	−142.8
3.30	−416.9	−353.9	−238.2	−158.9	−138.0	−126.1	−120.5	−119.0	−122.7	−130.5	−137.6	−144.3
3.40	−382.9	−327.8	−225.2	−153.8	−134.7	−123.9	−118.7	−117.2	−120.1	−125.9	−131.0	−133.1
3.50	−344.8	−297.1	−207.5	−144.4	−127.2	−117.5	−112.7	−111.3	−113.6	−117.9	−121.5	−122.8
3.60	−305.8	−265.1	−187.8	−132.4	−117.3	−108.7	−104.5	−103.3	−104.9	−108.1	−110.6	−111.7
3.80	−234.0	−204.7	−148.3	−107.0	−95.6	−89.0	−85.7	−84.7	−85.6	−87.4	−88.6	−89.0
4.00	−175.3	−154.4	−113.9	−83.6	−75.1	−70.2	−67.8	−67.0	−67.6	−68.7	−69.2	−69.4
4.50	−82.9	−74.2	−56.7	−43.0	−39.0	−36.7	−35.7	−35.3	−35.5	−36.0	−36.1	−36.2
5.00	−40.4	−36.5	−28.6	−22.2	−20.2	−19.3	−18.7	−18.5	−18.9	−19.1	−19.3	−19.3
5.50	−20.8	−19.0	−15.0	−12.0	−11.0	−10.5	−10.1	−10.1	−10.5	−10.7	−10.8	−10.8

[a] All energy values are in μE_h.

TABLE 2: Interaction Energies (in μE_h) and, in Parentheses, the Corresponding Equilibrium Intermolecular R_e Distances (in Å) Obtained from the ab Initio Results at Different Levels of Theory

	$\Theta = 0°$				$\Theta = 180°$			
basis set	UMP2	UMP3	UMP4	CCSD(T)	UMP2	UMP3	UMP4	CCSD(T)
aug-cc-pVDZ	−201.5 (3.43)	−232.4 (3.40)	−278.3 (3.36)		−56.3 (3.54)	−68.1 (3.52)	−80.0 (3.47)	
d-aug-cc-pVDZ	−212.9 (3.38)	−241.6 (3.35)	−287.2 (3.31)		−68.9 (3.51)	−84.7 (3.48)	−102.9 (3.36)	
aug-cc-pVTZ	−313.8 (3.23)	−356.9 (3.22)	−426.7 (3.15)		−78.7 (3.48)	−102.3 (3.46)	−119.7 (3.34)	
d-aug-cc-pVTZ	−320.9 (3.22)	−369.2 (3.20)	−437.1 (3.14)		−86.7 (3.42)	−114.2 (3.38)	−134.8 (3.19)	
aug-cc-pVTZ+bf	−329.7 (3.22)	−371.3 (3.19)	−446.6 (3.13)	−456.9 (3.12)	−94.8 (3.34)	−117.5 (3.28)	−142.9 (3.21)	−147.6 (3.21)
aug-cc-pVQZ	−334.7 (3.20)	−375.8 (3.18)	−449.8 (3.13)	−460.4 (3.13)	−88.9 (3.34)	−111.5 (3.29)	−134.6 (3.22)	−139.3 (3.22)
CBS[a]			−454.06				−143.55	

[a] The complete basis set limit was calculated from UMP4/aug-cc-pVnZ values (n = D, T, Q).

aug-cc-pVTZ + bf. To check the effects of the basis set on interaction energy calculations, we have performed also calculations with the (d-)aug-cc-pVnZ (n = D, T, Q) basis sets[68,69] on the selected geometries. All electrons were correlated in the supermolecular and intermolecular perturbation calculations. The spin contamination was negligible in all calculated points because the $\langle S^2 \rangle = 0.750$ corresponds to the exact value in the radical monomer as well as in the dimer.

4. Results and Discussion

A. Features of the PES. The investigation of the PES within the aug-cc-pVTZ+bf basis sets was carried out for the distances R in the range from 2.5 to 5.5 Å and for angles Θ ranging from 0° to 180°. The computed PES has two local minima (see Table 1 and Figure 1). The primary minimum occurs for the linear geometry $\theta = 0°$ at $R = 3.13$ Å, and its well depth (D_e) is 446.6 μE_h (98.01 cm^{-1}; see Table 2). These values are in agreement with the ab initio results of Stark and Werner[36] computed at the MR−CI level of theory. They found a minimum for the linear geometry at $R = 3.09$ Å with a well depth of about 446.2 μE_h (97.93 cm^{-1}). Our potential can be compared also with semiempirical 6SEC surface of Mielke et al.[35] Their PES shows a minimum at $R = 3.34$ Å with the well depth of 589.6 μE_h (129.41 cm^{-1}), which is slightly underestimated in comparison with the well depth found in this work, and the minimum occurs also at a longer distance.

There is also a secondary minimum of $C_{\infty v}$ symmetry which was found for the opposite H···FH orientation at $R = 3.21$ Å. Its well depth is estimated to 142.9 μE_h (31.36 cm^{-1}). The transition state, separating the two minima, is located at $R =$ 3.17 Å and $\Theta = 99°$ with the energy difference 372.4 μE_h (81.73 cm^{-1}) above the primary minimum. It should be noted that the above-mentioned two stationary points were not found on the PESs of Mielke[35] or Stark.[36]

Within the supermolecular calculations, the truncation effect of the correlation treatment on the values of interaction energies is important. Its role is illustrated in the first rows of the Table 3. The dominant part of the interaction correlation energy naturally originates from the values computed at the UMP2 level of theory. Although the contributions of $\Delta E^{(3)}(\Delta E_{int}^{(3)} - \Delta E_{int}^{(2)})$ and of $\Delta E^{(4)}(\Delta E_{int}^{(4)} - \Delta E_{int}^{(3)})$ are smaller (cca 10−16% with respect to the $\Delta E^{(2)}$ value), they significantly affect the value of the interaction energies (cf. Tables 2 and 3).

To check the reliability of the above-discussed results, Table 2 lists the equilibrium distances (R) and interaction energies for the minima, calculated with the (d-)aug-cc-pVnZ (n = D, T, Q) basis sets. The values obtained within the aug-cc-pVTZ basis sets extended by midbond functions are comparable with those obtained from the aug-cc-pVQZ basis set. The differences of the well depths obtained at the various UMP levels are ranging from 4 to 9 μE_h and for the equilibrium distances are maximally 0.02 Å. The interaction energies calculated using the CCSD(T) method for the aug-ccpVTZ+bf and aug-cc-pVQZ basis sets appear to be deeper when compared with the UMP values. However, the differences between the UMP4 and CCSD-(T) results for a given basis set are not so significant, the calculated energies in the vicinity of the minima differ only ±5%. A good correspondence between the supermolecular fourth-order perturbation theory and the coupled clusters results was published for other vdW complexes, too. For example, the

TABLE 3. Interaction Energies of the HF($X^1\Sigma_g^+$)−H(^2S) Complex[a]

	$R = 3.1$ Å, $\Theta = 0°$		$R = 3.2$ Å, $\Theta = 180°$	
energy	aug-cc-pVTZ	aug-cc-pVTZ+bf	aug-cc-pVTZ	aug-cc-pVTZ+bf
ΔE^{UHF}	211.1	206.2	116.1	117.6
$\Delta E^{(2)}$	−503.5	−519.4	−181.9	−205.7
$\Delta E_{int}^{(2)}$	−292.4	−313.2	−65.8	−88.1
$\Delta E^{(3)}$	−49.3	−46.8	−25.5	−27.1
$\Delta E_{int}^{(3)}$	−341.7	−360.0	−91.3	−115.2
$\Delta E^{(4)}$	−83.0	−85.5	−23.9	−27.6
$\Delta E_{int}^{(4)}$	−424.7	−445.5	−115.2	−142.8
ΔE^{HL}	964.8	964.0	177.9	180.8
$E_{els}^{(100)}$	−114.2	−115.0	−98.5	−96.8
ΔE_{def}^{HF}	−753.7	−757.8	−61.8	−63.2
$E_{ind}^{(200)}$	−629.4	−632.8	−106.3	−107.2
$E^{(200)}$	256.5	258.4	−84.7	−85.2
$E_{els}^{(12)}$	−42.8	−42.7	−36.8	−45.9
$E_{disp}^{(200)}$	−529.9	−546.1	−231.4	−259.8
$E_{exch-disp}^{(200)}$	62.1	66.1	24.7	28.4
$\Delta E_{other}^{(2)}$	7.1	3.3	61.6	71.6
$E_{disp}^{(210)} + E_{disp}^{(201)}$	30.3	27.3	25.5	24.8
$E_{disp}^{(300)}$	26.4	33.6	2.4	7.1

[a] All energy values are in μE_h.

recent ab initio data[71−74] for the water dimer reveal that the MP4 and CCSD(T) electron-correlation contributions to the interaction energy are very similar (within 3%) for the investigated orientations of the monomers.

Another problem is the saturation of the basis set. It has been observed previously[75−77] that the interaction energies computed with the correlation consistent basis sets appear to converge toward the "complete basis set" (CBS) limits. The convergence behavior is often described by the following simple exponential function[76]

$$A(n) = A(\infty) + Be^{-Cn} \tag{5}$$

where n is the cardinal number of the basis set ($n = 2$ for DZ, $n = 3$ for TZ, and so on), $A(\infty)$ is the estimated CBS limit, and B and C are adjustable parameters. The CBS limits, included in Table 2, were calculated from UMP4/aug-cc-pVnZ ($n = 2$, 3, 4) interaction energies. It can be seen that the computed values are very similar to CCSD(T)/aug-cc-pVQZ values.

B. Partitioning of the Interaction Energies. The next goal of this study was to discuss the physical origin of the stability of the studied vdW structures. Using the decomposition of the supermolecular UMP2 interaction energy, we can analyze and estimate how the fundamental components determine its anisotropy in the region near 3.1 Å. These dependencies are shown in Figures 2 and 3.

The UHF interaction energies (ΔE^{UHF}) display a weak angular dependence. In the linear arrangements, the interaction energy curves show minima, whereas the 30−60° region corresponds to a maximum. The positive value of this term is a consequence of the repulsive character of the HL exchange−penetration energy contributions (ΔE_{exch}^{HL}) included in the ΔE^{HL} energy. The attractive Coulombic forces are represented by the UHF electrostatic term ($E_{els}^{(100)}$). The UHF deformation term (ΔE_{def}^{UHF}) shows a reciprocal character to the HL anisotropy and has a strong smoothing effect on the total SCF interaction energy around the linear H···HF configuration. The origin of the large ΔE_{def}^{UHF} energy around $\Theta = 0°$ is also quite interesting. The

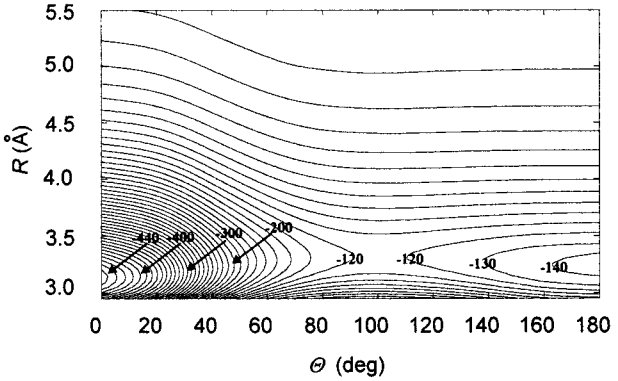

Figure 1. Contour plot of the interaction potential calculated at the UMP4/aug-cc-pVTZ+bf level of theory. The contour spacing is 10 μE_h.

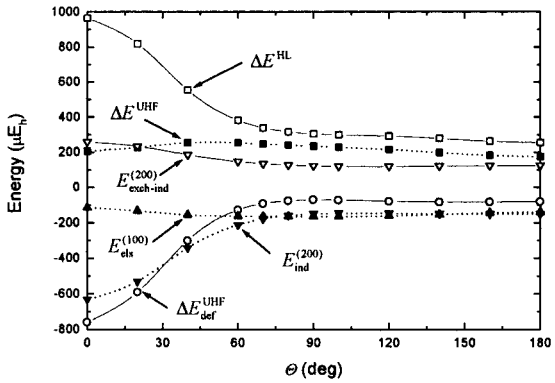

Figure 2. Angle dependence of the UHF/ aug-cc-pVTZ+bf interaction energy and its components for HF($X\ ^1\Sigma_g^+$)−H(^2S) at $R = 3.1$ Å.

dominant part of this energy represents the UHF induction term ($E_{ind}^{(200)}$) which describes the classic charge induction. As we can see from the Table 3, the induction interaction between the partially positively charged H in the polar HF molecule and the neutral H atom around the first vdW minimum is approximately three-times stronger than that in the second case. On the other hand, the relevant exchange−penetration coun-

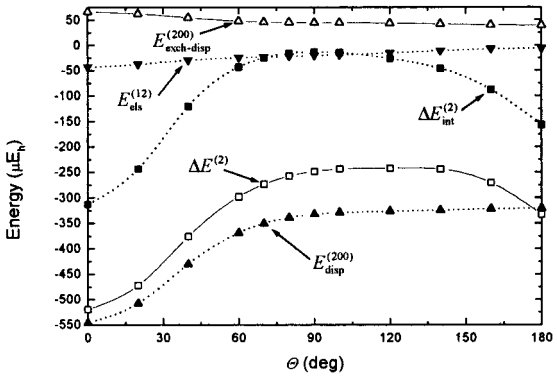

Figure 3. Angle dependence of the UMP2/ aug-cc-pVTZ+bf interaction energy and its components for HF(X $^1\Sigma_g^+$)−H(^{2}S) at $R = 3.1$ Å.

terpart displays not so strong dependence on the geometrical orientation (see Figure 2).

Similarly, $\Delta E^{(2)}$ plays an important role in forming the shape of the total UMP2 interaction energy curves. The $E_{\mathrm{disp}}^{(200)}$ is the dominant attractive contribution within the interaction correlation energy (see Table 3). A comparison of the interaction energy components calculated within the aug-cc-pVTZ and aug-cc-pVTZ+bf basis sets indicates that the extension of basis set affects primarily the dispersion energies. Other calculated attractive term represents the electrostatic correlation energy ($E_{\mathrm{els}}^{(12)}$) which tends to zero at the linear H···FH form. It is suitable to point out that the other exchange−penetration deformation energies as well as the response effects collected in the $\Delta E_{\mathrm{other}}^{(2)}$ term are negligible at $\Theta = 0°$.

The Table 3 also provides the higher-order dispersion corrections ($E_{\mathrm{disp}}^{(210)}$, $E_{\mathrm{disp}}^{(201)}$, and $E_{\mathrm{disp}}^{(300)}$) which appear in the third-order interaction correlation energy ($\Delta E^{(3)}$). Their sum is positive, and it is evident that the electrostatic correlation and relevant correlation−deformation contributions will dominate in $\Delta E^{(3)}$.

C. Surface Fit. The calculated potential energy points were fitted to the following general functional form containing the short-range part, V_{sh}, and the asymptotic long-range part, V_{as}:

$$\Delta E_{\mathrm{int}}(R,\Theta) = V_{\mathrm{sh}}(R,\theta) + V_{\mathrm{as}}(R,\theta) \tag{6}$$

where

$$V_{\mathrm{sh}}(R,\theta) = G(R,\theta)\exp\left(D(\theta) + B(\theta)\frac{R}{q}\right) \tag{7}$$

$G(R,\theta)$, $D(\theta)$, and $B(\theta)$ were expanded in associated Legendre polynomials up to the order $l = 6$:

$$G(R,\theta) = \sum_{l=0}^{6}\frac{P_l^{\,0}(\cos\theta)}{\sqrt{2l+1}}\sum_{k=0}^{4} g_k^l\left(\frac{R}{q}\right)^k \tag{8}$$

$$D(\theta) = \sum_{l=0}^{6} d_l P_l^{\,0}(\cos\theta) \tag{9}$$

$$B(\theta) = \sum_{l=0}^{6} b_l P_l^{\,0}(\cos\theta) \tag{10}$$

The asymptotic part includes a standard damped-dispersion expression, which is truncated at the six power of inverse R:

$$V_{\mathrm{as}}(R,\theta) = \frac{f_6\left[B(\theta)\frac{R}{q}\right]}{\left(\frac{R}{q}\right)^6}\sum_{l=0}^{2}\frac{C_l}{\sqrt{2l+1}}P_l^{\,o}(\cos\theta) \tag{11}$$

where the $f_6(x)$ term denotes the damping function of Tang and Toennies[78] defined by

$$f_6(x) = 1 - \mathrm{e}^{-x}\sum_{k=0}^{6}\frac{x^k}{k!} \tag{12}$$

A rigorous least-squares fitting procedure was used to determine all 53 variational parameters (Table 4). Prior to the least-squares calculation, the original grid of 216 potential energy points has been expanded by the bicubic spline interpolation procedure[79] to 2220 points. The average absolute deviation between the original points and the fit was smaller than 0.81 μE_h (0.18 cm^{-1}). The quality of the fit was also tested by the calculation of 100 randomly selected points. The average absolute deviation of these tested points was 0.64 μE_h (0.14 cm^{-1}).

D. Bound State Calculations. The energies of bound states were determined by the coupled-channel approach with the BOUND program of Hutson.[80] The Hamiltonian used in BOUND has the following form:

$$\hat{H} = -\frac{\hbar^2}{2\mu}R^{-1}\frac{\mathrm{d}^2}{\mathrm{d}R^2}R + \hat{H}_{\mathrm{int}} + V(R,\Theta) \tag{13}$$

where R and Θ denote the Jacobi coordinates defined earlier, $\hat{H}_{\mathrm{int}}$ denotes the sum of internal Hamiltonians of the isolated HF and H, and $V(R,\Theta)$ denotes the intermolecular potential. In the coupled-channel method, the radial coordinate (R) was handled using a grid, whereas the angular coordinate (Θ) was handled using a basis set. In the basis set expansion, the channels up to $j = 20$ have been included, and the resulting coupled equations were solved using the log−derivative propagator of Manolopoulos.[81] The coupled equations were propagated from $R_{\mathrm{min}} = 1.0$ Å to $R_{\mathrm{max}} = 8.0$ Å, extrapolating to zero step size from log−derivative interval sizes of 0.01 and 0.02 Å using Richardson h^4 extrapolation. For our calculations, we used the following input parameters: the rotational constant of HF $b = 20.5597$ cm^{-1} and the reduced mass of the H···HF complex $\mu = 0.959\,49$ amu.

A complete treatment of the dynamics on the studied system would require us to include the spin of the hydrogen atom in calculating the ro-vibrational energy levels. However, the main object of the present work is to determine only the qualitative characteristics of the vibrational energy-level pattern; therefore, the influence of such effects is neglected.

Although for three-body systems the dynamical calculations of ro-vibrational energy levels are nearly exact, it may be helpful to characterize the calculated states by approximate quantum numbers. First, we note that the HF vibrations can, to a very good approximation,[82] be decoupled from internal modes because of the high frequency of the HF stretching fundamental $\upsilon = 3961.4229$ cm^{-1} (ref 83). The remaining internal ro-vibrational states are assigned following the notation of Meuwly et al.[84] by the total angular momentum quantum number J, its projection K onto the molecule fixed z axis, a bending quantum number υ_b, which correlates in the isotropic limit with the HF rotational quantum number j, and the vdW stretching quantum number υ_s. If the nodal structure of the wave function is regular, υ_s and υ_b represent the number of the wave function nodes in

TABLE 4: Parameters of the Analytical Potential Fit (eq 6) of Data Obtained from Table 1 (q = 8.458 534)

L	0	1	2	3	4	5	6
g_0^L	−0.132 024	0.033 262	0.012 522	−0.019 808	0.019 698	0.004 664	0.015 863
g_1^L	0.790 390	−0.209 488	−0.014 184	0.220 044	−0.096 970	−0.004 637	−0.173 735
g_2^L	−1.810 447	0.510 851	−0.127 972	−0.747 416	0.172 784	−0.063 745	0.605 903
g_3^L	1.868 937	−0.565 960	0.320 714	1.038 818	−0.126 419	0.166 400	−0.873 099
g_4^L	−0.730 529	0.238 819	−0.208 840	−0.518 107	0.028 743	−0.114 539	0.452 589
d_L	12.213 688	0.405 816	0.667 694	0.077 693	0.063 053	0.049 376	−0.029 795
b_L	1.488 782	−0.245 354	0.432 864	−0.956 139	−0.298 263	−0.000 387	0.074 685
C_L	2.773 392	1.274 503	2.909 721				

TABLE 5: Energies and Expectation Values for the Ground State and the Lowest Excited Bending and Stretching States

(υ_b υ_s K)	energy/cm^{-1}	($\langle 1/R^2\rangle$)$^{-}$1/2/Å	$\langle P_2(\cos\Theta)\rangle$
(0 0 1/2)	−21.01	3.31	0.98
(0 1 1/2)	−7.48	3.49	0.86
(0 2 1/2)	−3.71	3.53	0.85
(1 0 1/2)	−1.65	3.84	0.69
(0 0 3/2)	−18.17	3.37	0.95

the bend Θ and the stretch R coordinates, respectively. All states can be further assigned with the symmetry label $\epsilon = e$ or f which indicates the parity of the wave function. With respect to the above-mentioned notation, in the present work, a label (υ_b, υ_s, K) will characterize the ro-vibrational states.

The bound-state calculations reveal that the ground state is 21.01 cm^{-1} below dissociation to HF($^1\Sigma_g^+$) + H(^{2}S). The effect of the zero-point oscillation is clearly large, because more of the half of the well depth is consumed by zero-point energy. The average distance of the hydrogen atom to the center of mass of HF is 3.31 Å, which is roughly 0.2 Å larger than the equilibrium separation of the primary minimum. Because the global minimum of PES is at $\Theta = 0°$, we expect that the lowest energy states will be the ones that have the largest probability at $\Theta = 0°$. As a matter of fact, the ground state is concentrated in the vicinity of the global minimum as signalized by the mean value of the Legendre polynomial $\langle P_2(\cos\Theta)\rangle$ =0.98. (The value $\cos^{-1}[(2\langle P_2(\cos\Theta)\rangle + 1)/3]^{1/2}$ indicates the angular extent of the wave function.) The expectation value $\langle 1/R^2\rangle$ and the wave function calculated in the helicity decoupled approximation show that the first excited $J = {}^1/_2$ state is the vdW stretch $\upsilon_s = 1$ (0 1 $^1/_2$). It lies about 14 cm^{-1} higher in energy than the ground state. Because of the rather flat PES, this state already probes a much larger radial range than (0 0 $^1/_2$) as can be seen from the results listed in Table 5. However, the state is still concentrated around the linear configuration, suggested by the expectation value $\langle P_2(\cos\Theta)\rangle = 0.86$. The next fundamental (1 0 $^1/_2$) appears approximately 19 cm^{-1} above the ground state (0 0 $^1/_2$) and is sensitive to a rather large part of the PES. The radial average is more than 3.8 Å, and the structure is far from the linear geometry. The $K = {}^3/_2$ excitation of (0 0 $^1/_2$) is 3 cm^{-1} higher in energy. This state has a node in the linear configuration and a behavior similar to (0 0 $^1/_2$). The vibrational energy levels of H−HF complex are collected in Figure 4. The density of states is rather low, and no bound states exist for $K > {}^5/_2$.

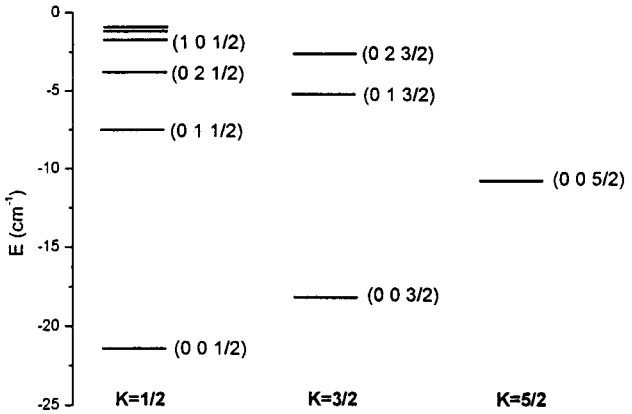

Figure 4. Bound states for the HF(X $^1\Sigma_g^+$)−H(^{2}S) complex. Only states with $J = K^+$ are shown.

5. Conclusions

The ab initio PES for the HF(X $^1\Sigma_g^+$)−H(^{2}S) interaction was evaluated at the UMP4 level and analyzed by dissecting the UMP2 and UMP3 interaction energies into four fundamental components. The first minimum occurs for the linear geometry H···HF. The well depth interpolated from an analytical fit is 98.01 cm^{-1} at $R_e = 3.13$ Å. The best computed value is 101.04 cm^{-1} at the CCSD(T)/aug-cc-pVQZ level of theory. The resulting well depth is expected to be accurate within a few percent. The well depth of a local minimum for the collinear geometry interpolated from the fit amounts to 31.36 cm^{-1} at $\Theta = 180°$ and $R_e = 3.21$ Å, whereas the lowest computed point for $R = 3.22$ Å gives the estimate of 32.39 cm^{-1} at the CCSD-(T)/aug-cc-pVTZ+bf level of theory. Further improvement of the PES at the used electron-correlation level can be achieved by extensive calculations (using correlation consistent basis sets extended with series of bond functions[71]) of its individual points and their extrapolation toward the CBS limits.

The ground vibrational state calculated by means of close-coupled equations is localized in the global minimum and gives the dissociation energy $D_0 = 21.01$ cm^{-1}. The calculated average value of R in the ground state is 3.31 Å.

A decomposition of the interaction energy applicable to open-shell systems was also done. The interaction energies were dissected into four fundamental components—electrostatic, exchange-penetration, induction, and dispersion—having a similar physical interpretation as in the case of the closed-shell species.[54−59] The analysis of these components reveals that the UHF interaction energies calculated for the linear arrangements are practically determined by the repulsive HL energy and attractive induction energy included in the ΔE_{def}^{UHF} term. In investigated geometries, the $\Delta E^{(2)}$ energy is dominated by the attractive $E_{disp}^{(200)}$ energy. However, in the $\Delta E^{(3)}$ energy, the electrostatic correlation and the relevant correlation−deformation effects play an important role.

Acknowledgment. Dedicated to Professor V. Kvasnička on the occasion of his 60th birthday. This work was supported by the Slovak Scientific Grant Agency (Projects Nos. 1/7355/20 and 1/7388/20).

References and Notes

(1) Leopold, K. R.; Fraser, G. T.; Novick, S. E.; Klemper, W. *Chem. Rev.* **1994**, *94*, 1807.
(2) Nesbitt, D. J. *Annu. Rev. Phys. Chem.* **1994**, *45*, 367.
(3) Cohen, R. C.; Saykally, R. J. *J. Phys. Chem.* **1992**, *96*, 1024.

(4) Hutson, J. M. *Annu. Rev. Phys. Chem.* **1990**, *41*, 123.
(5) Bacic, Z.; Miller, R. E. *J. Phys. Chem.* **1996**, *100*, 12945.
(6) Furio, N.; Ali, A.; Dagdigian, P. J. *Chem. Phys. Lett.* **1986**, *125*, 561.
(7) Furio, N.; Ali, A.; Dagdigian, P. J. *J. Chem. Phys.* **1986**, *85*, 3860.
(8) Jihua, G.; Ali, A.; Dagdigian, P. J. *J. Chem. Phys.* **1986**, *85*, 7098.
(9) Ali, A.; Jihua, G.; Dagdigian, P. J. *J. Chem. Phys.* **1987**, *87*, 2045.
(10) Randall, R. W.; Chuang, C.-C.; Lester, M. J. *Chem. Phys. Lett.* **1992**, *200*, 113.
(11) Heaven, M. C. *J. Chem. Phys.* **1993**, *97*, 8567.
(12) Qian, H.-B.; Seccombe, D.; Howard, B. J. *J. Chem. Phys.* **1997**, *107*, 7685.
(13) Meuwly, M.; Hutson, J. M. *J. Chem. Phys.* **2000**, *112*, 592.
(14) Carter, C. C.; Miller, T. A. *J. Chem. Phys.* **1997**, *107*, 3447.
(15) Dubernet, M.-L.; Hutson, J.-M. *J. Chem. Phys.* **1993**, *99*, 7477.
(16) Chang, B.-C.; Yu, L.; Cullin, D.; Refuss, B.; Williamson, J.; Miller, T. A.; Fawzy, W. M.; Zheng, X.; Fei, S.; Heaven, M. C. *J. Chem. Phys.* **1991**, *95*, 7086.
(17) Chuang, C.-C.; Andrews, P. M.; Lester, M. I. *J. Chem. Phys.* **1995**, *103*, 3418.
(18) Lawrence, W. G.; Chen, Y.; Heaven, C. M. *J. Chem. Phys.* **1997**, *107*, 7163.
(19) Halpern, J. B.; Huong, Y.; Titauchuk, T. *Astrophys. Space Sci.* **1996**, *236*, 11.
(20) Mulliken, R. S. *J. Chem. Phys.* **1964**, *61*, 20.
(21) Rebentrost, F.; Lester, W. A., Jr. *J. Chem. Phys.* **1975**, *63*, 3737.
(22) Airey, J. R. *Int. J. Chem. Kinet.* **1970**, *2*, 65.
(23) Neumark, D. M.; Wodtke, A. M.; Robinson, G. N.; Hayden, G. N.; Lee, Y. T. *J. Chem. Phys.* **1985**, *82*, 3045.
(24) Neumark, D. M.; Wodtke, A. M.; Robinson, G. N.; Hayden, G. N.; Shobatake, R.; Sparks, R. K.; Schafer, T. P.; Lee, Y. T. *J. Chem. Phys.* **1985**, *82*, 3067.
(25) Faubel, M.; Rusin, L. Y.; Sondermann, F.; Schlemmer, S.; Tappe, U.; Toennies, J. P. *J. Chem. Phys.* **1994**, *101*, 2106.
(26) Baer, M.; Faubel, M.; Martínez-Haya, B.; Rusin, L. Y.; Tappe, U.; Toennies, J. P. *J. Chem. Phys.* **1998**, *108*, 9694.
(27) Faubel, M.; Martinez-Haya, B.; Rusin, L. Y.; Tappe, U.; Toennies, J. P.; Aoiz, F. J.; Bañares, L. *J. Phys. Chem. A* **1998**, *102*, 8695.
(28) Bradforth, S. E.; Arnold, D. W.; Neumark, D. M.; Manolopoulos, D. E. *J. Chem. Phys.* **1993**, *99*, 6345.
(29) Manolopoulos, D. E.; Stark, K.; Werner, H.-J.; Arnold, D. W.; Bradforth, S. E.; Neumark, D. M. *Science* **1993**, *262*, 1852.
(30) Chapman, W. B.; Blackmon, B. W.; Nesbitt, D. J. *J. Chem. Phys.* **1997**, *107*, 8193.
(31) Chapman, W. B.; Blackmon, B. W.; Nizkorodov, S.; Nesbitt, D. J. *J. Chem. Phys.* **1998**, *109*, 9306.
(32) Dharmasena, G.; Philips, T. R.; Shokhirev, K. N.; Parker, G. A.; Keil, M. *J. Chem. Phys.* **1997**, *106*, 9950.
(33) Dharmasena, G.; Copeland, K.; Young, J. H.; Lasell, R. A.; Phillips, T. R.; Parker, G. A.; Keil, M. J. *J. Phys. Chem.* **1997**, *106*, 9950.
(34) Lynch, G. C.; Steckler, R.; Schwenke, D. W.; Varandas, A. J. C.; Truhlar, D. G. *J. Chem. Phys.* **1991**, *94*, 7136.
(35) Mielke, S. L.; Lynch, G. C.; Truhlar, D. G.; Schwenke, D. W. *Chem. Phys. Lett.* **1993**, *213*, 11.
(36) Stark, K.; Werner, H.-J. *J. Chem. Phys.* **1996**, *104*, 6515.
(37) Hartke, B.; Werner, H.-J. *Chem. Phys. Lett.* **1997**, *280*, 430.
(38) Maierle, C. S.; Schatz, G. C.; Gordon, M. S.; McCabe, P.; Connor, J. N. L. *J. Chem. Soc. Faraday Trans.* **1997**, *93*, 709.
(39) Takayanagi, T.; Kurosaki, Y. *J. Chem. Phys.* **1998**, *109*, 8929.
(40) Takayanagi, T.; Kurosaki, Y. *Chem. Phys. Lett.* **1998**, *286*, 35.
(41) Dobbyn, A. J.; Connor, J. N. L.; Besley, N. A.; Knowles, P. J.; Schatz, G. C. *Phys. Chem. Chem. Phys.* **1999**, *1*, 957.
(42) Dubernet, M.-L.; Hutson, J.-M. *J. Phys. Chem.* **1994**, *98*, 5844.
(43) Klos, J.; Chalasinski, G.; Berry, M. T.; Kendall, R. A.; Burcl, R.; Szczesniak, M.; Cybulski, S. M. *J. Chem. Phys.* **2000**, *112*, 4952.
(44) van Duijneveldt, F. B.; van Duijneveldt-van de Rijdt, J. G. C. M.; van Lenthe, J. H. *Chem. Rev.* **1994**, *94*, 1873.
(45) Boys, S. F.; Bernardi, F. *Mol. Phys.* **1970**, *19*, 553.
(46) Chalasinski, G.; Szczeszniak, M. M. *Chem. Rev.* **2000**, *100*, 4227 and references therein.
(47) Cybulsky, S. M.; Burcl, M.; Chalasinski, G.; Szczeszniak, M. M. *J. Chem. Phys.* **1996**, *104*, 7997.
(48) Lukeš, V.; Laurinc, V.; Biskupič, S. *J. Comput. Chem.* **1999**, *20*, 857.
(49) Kendal, R. A.; Chalasinski, G.; Klos, J.; Bukowski, R.; Severson, M. W.; Szczesniak, M. M.; Cybulski, S. M. *J. Chem. Phys.* **1998**, *108*, 3235.
(50) Cybulski, S. M.; Chalasinski, G.; Szczesniak, M. M. *J. Chem. Phys.* **1996**, *105*, 9525.
(51) Burcl, R.; Krems, R. V.; Buchachenko, A. A.; Szczesniak, M. M.; Chalasinski, G.; Cybulski, S. M. *J. Chem. Phys.* **1998**, *109*, 2144.
(52) Vrábel, I.; Lukeš, V.; Laurinc, V.; Biskupič, S. *J. Phys. Chem. A* **2000**, *104*, 96.
(53) Lukeš, V.; Bittererová, M.; Laurinc, V.; Biskupič, S. *Chem. Phys.* **2000**, *257*, 157.
(54) Rybak, S.; Jeziorski, B.; Szalewicz, K. *J. Chem. Phys.* **1991**, *95*, 6576.
(55) Moszyński, R.; Heijmen, T. G. A.; Jeziorski, B. *Mol. Phys.* **1996**, *88*, 741.
(56) Jeziorski, B.; Moszynski, R.; Ratkiewicz, A.; Rybak, S.; Szalewicz, K.; Williams, H. L. SAPT: A program for Many-body Symmetry-Adapted Perturbation Theory Calculations of Intermolecular Interaction Energies. In *Methods and Techniques in Computational Chemistry: METECC-94 Vol B*; Clementi, E., Ed.; STEF: Cagliari, Italy, 1993.
(57) Surján, P. R.; del Valle, C. P.; Lain, L. *Int. J. Quantum Chem.* **1997**, *64*, 43 and references therein.
(58) Laurinc, V.; Lukeš, V.; Biskupič, S. *Theor. Chim. Acc.* **1998**, *99*, 53 and references therein.
(59) Lukeš, V.; Laurinc, V.; Biskupič, S. *Int. J. Quantum Chem.* **1999**, *20*, 857 and references therein.
(60) Löwdin, P.-O. *Adv. Phys.* **1956**, *5*, 1.
(61) Jeziorski, B.; van Hemert, N. C. *Mol. Phys.* **1976**, *31*, 713.
(62) Salter, E. A.; Trucks, G. W.; Bartlett, R. J. *J. Chem. Phys.* **1980**, *90*, 1752 and references therein.
(63) Cybulski, S. M. *J. Chem. Phys.* **1992**, *97*, 7545 and references therein.
(64) Moszyński, R.; Jeziorski, B.; Ratkiewicz, A.; Rybak, S. *J. Chem. Phys.* **1993**, *99*, 8856.
(65) Kochanski, E. *J. Chem. Phys.* **1973**, *58*, 5823.
(66) Frisch, M. J.; Trucks, G. W.; Schlegel, H. B.; Gill, P. M. W.; Johnson, B. G.; Robb, M. A.; Cheeseman, J. R.; Keith, T.; Petersson, G. A.; Montgomery, J. A.; Raghavachari, K.; Al-Laham, M. A.; Zakrzewski, V. G.; Ortiz, J. V.; Foresman, J. B.; Cioslowski, J.; Stefanov, B. B.; Nanayakkara, A.; Challacombe, M.; Peng, C. Y.; Ayala, P. Y.; Chen, W.; Wong, M. W.; Andres, J. L.; Replogle, E. S.; Gomperts, R.; Martin, R. L.; Fox, D. J.; Binkley, J. S.; Defrees, D. J.; Baker, J.; Stewart, J. P.; Head-Gordon, M.; Gonzalez, C.; Pople, J. A. *Gaussian 94*; Gaussian, Inc.: Pittsburgh, PA, 1995.
(67) Huber, K. P.; Herzberg, G. *Molecular Spectra and Molecular Structure IV. Constants of Diatomic Molecules*; Van Nostrand Reinhold: New York 1979.
(68) Dunning, T. H., Jr. *J. Chem. Phys.* **1989**, *90*, 1007.
(69) Kendall, R. A.; Dunning, T. H., Jr.; Harrison, R. J. *J. Chem. Phys.* **1992**, *96*, 6796.
(70) Tao, F.-M.; Pan, Y.-K. *J. Chem. Phys.* **1992**, *97*, 4989.
(71) Torheyden, M.; Jansen, G. *Theor. Chem. Acc.* **2000**, *104*, 370.
(72) Mas, E. M.; Szalewicz, K.; Bukowski, R.; Jeziorski, B. *J. Chem. Phys.* **1997**, *107*, 4207.
(73) Schütz, M.; Brdarsk, S.; Widmark, P. O.; Lindh, R.; Karlströ, G. *J. Chem. Phys.* **1997**, *107*, 4597.
(74) Halkier, A.; Koch, H.; Jørgensen, P.; Christiansen, O.; Beck Nielsen, I. M.; Helgakar, T. *Theor. Chem. Acc.* **1997**, *97*, 150.
(75) Peterson, K. A.; Dunning, T. H., Jr. *J. Chem. Phys.* **1995**, *102*, 2032.
(76) Feller, D. J. *J. Chem. Phys.* **1992**, *96*, 6104.
(77) Xantheas, S. S.; Dunning, T. H., Jr. *J. Chem. Phys.* **1993**, *97*, 18.
(78) Tang, K. T.; Toennies, J. P. *J. Chem. Phys.* **1984**, *80*, 3726.
(79) Engels-Müllges, G.; Uhlig, F. *Numerical Algorithms with FORTRAN*; Springer: Berlin, 1996.
(80) Hutson, J. M. *BOUND* computer program, version 5; distributed by Collaborative Computational Project No. 6 of the U.K. Engineering and Physical Sciences Research Council, 1996.
(81) Manolopoulos, D. E. *J. Chem. Phys.* **1986**, *85*, 6425.
(82) Tennyson, J.; Sutcliffe, B. T. *J. Chem. Phys.* **1983**, *79*, 43.
(83) Guelachvili, G. *Opt. Commun.* **1976**, *19*, 150.
(84) Meuwly, M.; Wright, N. J. *J. Phys. Chem. A* **2000**, *104*, 1271.